

DNA Origami-Enabled Plasmonic Sensing

Mihir Dass, Fatih N. Gür, Karol Kołtąj, Maximilian J. Urban, and Tim Liedl*



Cite This: *J. Phys. Chem. C* 2021, 125, 5969–5981



Read Online

ACCESS |

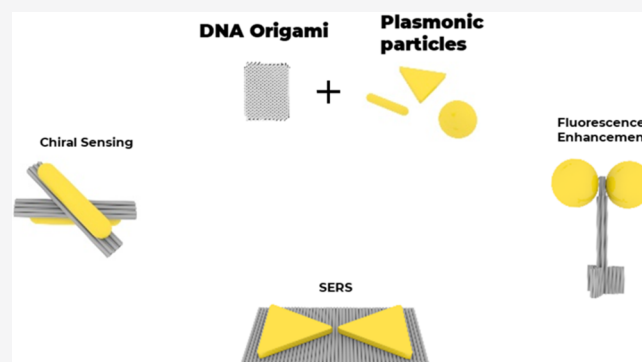


Metrics & More



Article Recommendations

ABSTRACT: The reliable programmability of DNA origami makes it an extremely attractive tool for bottom-up self-assembly of complex nanostructures. Utilizing this property for the tuned arrangement of plasmonic nanoparticles holds great promise particularly in the field of biosensing. Plasmonic particles are beneficial for sensing in multiple ways, from enhancing fluorescence to enabling a visualization of the nanoscale dynamic actuation via chiral rearrangements. In this Perspective, we discuss the recent developments and possible future directions of DNA origami-enabled plasmonic sensing systems. We start by discussing recent advancements in the area of fluorescence-based plasmonic sensing using DNA origami. We then move on to surface-enhanced Raman spectroscopy sensors followed by chiral sensing, both utilizing DNA origami nanostructures. We conclude by providing our own views on the future prospects for plasmonic biosensors enabled using DNA origami.



INTRODUCTION

The ability to sense external or internal stimuli is a key feature of life. Indeed, sensing allows natural systems to adapt to environmental changes thus improving their chances of propagation. In such systems, molecules detect changes in the environment, for example, concentration of nutrients or intensity of light irradiation, and turn them into biochemical stimuli. In medicine, the sensing of biomolecules is of great interest in clinical diagnostics to enable an early and low-concentration detection of disease biomarkers without the need for expensive equipment. Therefore, highly sensitive devices with simple readout capabilities are the need of the hour.

An ideal biomolecular sensor transduces a binding event into a strong output signal. In this work, we cover recent advances in plasmonic sensing using bottom-up fabricated DNA-based nanostructures. We will focus on assemblies of metallic nanoparticles that take advantage of optical near-field effects, in particular, electric field enhancement and plasmonic chirality. For the well-established sensors based on shifting surface plasmon resonances, we point the reader to the existing literature.^{1–3} Other, very recent, reviews cover related focus areas ranging from the interaction of DNA with pathogens to the use of DNA in nanophotonics.^{4–6}

Another established sensing scheme utilizing noble metal nanoparticles is the lateral flow assay. Here, the strong absorption and scattering capabilities of nanoparticles (AuNPs) play a key role along with reliable particle synthesis and conjugation methods to enable the easily visible bands on

test strips, an example being the severe acute respiratory syndrome coronavirus 2 (SARS-CoV-2) rapid antigen tests. However, these strips are limited in sensitivity and selectivity as well as the type of output signals (scattering and fluorescence color). Advances in nanofabrication, optical detection, and conjugation chemistry lead to the development of higher performance devices with more functional capabilities. Two such strategies are (i) biomolecular assays making use of plasmonic “hot-spots” and (ii) sensing enabled through a dynamic structural reconfiguration. Both of these sensing principles require an excellent control over molecular placement at the nanoscale. While a precise positioning of objects at the macroscopic scale is a trivial task, it is extremely challenging to achieve at the nanoscale. This is due to a combination of the effects of Brownian motion that prevails at such dimensions, a lack of tools to precisely manipulate nanoscale objects, as well as a lack of strategies capable of positioning multitudes of objects deterministically at the same time for a parallel assembly.

Among current nanofabrication strategies, DNA nanotechnology has emerged as one of the most successful. The description of the dynamic “Holliday junction” by Holliday⁷

Received: December 17, 2020

Revised: January 31, 2021

Published: February 25, 2021



led Seeman to design an immobile Holliday junction,⁸ kickstarting the use of DNA as a material and thus the field of DNA nanotechnology.^{9,10} Today, there are two main approaches to build bottom-up assembled DNA nanostructures. For the longest time, DNA structures were exclusively assembled from oligonucleotides, that is, synthetic DNA strands up to several tens of nucleotides long. Examples of this approach are “tile assembly” and “DNA bricks”.^{11–13} The second approach involves the use of a long scaffolding molecule and is widely known as (scaffolded) “DNA origami”.^{14–16} DNA origami structures are thus created from a “scaffold” strand that usually is of biological origin and multiple short, synthetic “staple” oligonucleotides. Consequently, each synthetic nucleotide can be easily customized to achieve an intended purpose. Analogous to a breadboard in electronics, various components can be placed at predefined positions to achieve structures that can perform programmed functions. Since its advent,¹⁵ the DNA origami technique has been used for the bottom-up assembly of functional structures aimed at a variety of uses, from a DNA “box” potentially capable of triggered drug-release¹⁷ to a controllable robotic arm at the nanoscale.¹⁸ This variety in application is driven by a molecular addressability that enables the placement of moieties with a resolution that is theoretically equal to the distance from base pair to base pair in a double helix, that is, 0.34 nm. Remarkably, also in experiments, position accuracy below 1 nm has been achieved with DNA self-assembly.^{19,20} Clearly, the strong functional capability of plasmonic DNA origami, the subject of this Perspective, relies on such a precise placement of plasmonic particles in user-defined configurations.

The attachment of plasmonic particles, most commonly gold, is achieved through a complementary base-pairing between DNA-covered nanoparticles and the DNA origami structure. Simply put, the surface of the plasmonic particle is functionalized with thiolated DNA oligonucleotides of a defined sequence. Specific staple strands of the origami structure are then extended with a sequence—we often refer to it as the “handle” sequence—that is complementary to the DNA on the plasmonic particles, the “anchor” sequences. The geometrical configuration of the handles on the origami defines the placement of the particles on the origami. Since each nucleotide’s position and sequence in the origami structure are deterministically known, the placement of particles can be controlled with the step size between two base pairs thus allowing sub-nanometer precision.

Mirkin et al. and Alivisatos et al. reported the first instances of using a thiol-capped DNA sequence to functionalize and arrange gold nanoparticles.^{21,22} Since then, thiolated DNA has become ubiquitous for functionalizing gold and other plasmonic nanoparticles. The gold–thiol bond is well-studied for its pseudocovalent nature leading to strong binding strengths. It is, however, challenging to achieve a high-density loading of DNA on colloidal particles due to its negatively charged phosphate backbone. A slow addition of salt (salt-aging) mitigates this by screening the charges on adjacent DNA oligonucleotides, allowing the DNA to pack closely on the surface of metal nanoparticles.^{23–26}

An alternative to this approach is the freeze–thaw method reported by Liu and Liu.^{27,28} The authors showed that freezing a solution containing AuNPs, DNA, and salt could help to speed up the conjugation process dramatically. The freezing results in ice crystals composed of pure water,

pushing the nonwater components into gaps between the crystals, where they reach saturated concentrations, allowing the DNA to efficiently bind to gold via its thiolated end. The robustness, simplicity, and rapidity of this technique can be instrumental both to be adopted by a wider scientific community as well as being easily transferable to industrial applications. We point readers to a review that discusses this and other attachment protocols in more detail.²⁹

Plasmonics coupled with DNA origami has opened up the opportunity to apply fundamentally new approaches to sensing. In this Perspective, we discuss recent advances in molecular sensing using plasmonic DNA origami structures, beginning with plasmon-enhanced fluorescence-based detection, followed by surface-enhanced Raman spectroscopy (SERS) sensing, and last, chiral plasmonic sensing. Finally, we will try to outline the major hurdles that must be overcome in the near future to expedite these advances, from accurate biomolecule detection using off-the-shelf products to the detection of analytes at the single-molecule level.

■ FLUORESCENCE-BASED PLASMONIC SENSING WITH DNA ORIGAMI

The structural arrangement of metal nanoparticles in the proximity of fluorophores can lead to a variety of physical effects, ranging from fluorescence enhancement (FE) over distance-dependent quenching to permanent photobleaching. Of these, FE holds special promise in the realm of biosensing and diagnostics. Plasmonic nanostructures can create highly localized electric fields, which can enhance the fluorescence of molecules in their vicinity.³⁰ The degree of enhancement is influenced by the size of the plasmonic particle (in a first approximation the larger the size, the higher the enhancement) and its shape (high-aspect-ratio nanorods or bipyramids can have strongly enhanced fields at their tips) as well as its chemical composition (e.g., silver leading to stronger plasmon coupling than gold).

The placement of metallic nanoparticles near fluorescent entities can affect the fluorescence emission in many ways: influencing the distance-dependent radiative and nonradiative decay rate and enhancing the local electric field as well as generally increasing the apparent cross section of small organic dyes with the help of comparatively large plasmonic antennas. As the nanoparticle diameter increases, the relative contribution of the scattering in the total extinction increases.³¹ This increase of the scattering cross section for larger particles has been suggested to account for a part of the FE, with a further contribution coming from the radiative rate enhancement.^{32,33} Control over the distance between the metallic nanoparticle and the fluorescent molecule is extremely crucial for influencing the radiative and nonradiative decay rates as shown by Acuna et al.^{34,35} and others.^{36–41} We will see below that FE effects can be enhanced over 5000-fold by placing two or more particles in close proximity, which leads to the creation of a plasmonic “hot-spot” between them due to the coupling of their respective electromagnetic fields.

An important aspect of achieving control over a particle placement on DNA origami is the DNA connector configuration. Generally, two connection strategies are available for binding AuNPs to a DNA origami structure: the shear and the zipper configuration. In the former, the same terminal ends (either both 5′ or both 3′ ends) of the handles and the anchors are protruding from their respective surface (gold or origami), and thus, after antiparallel

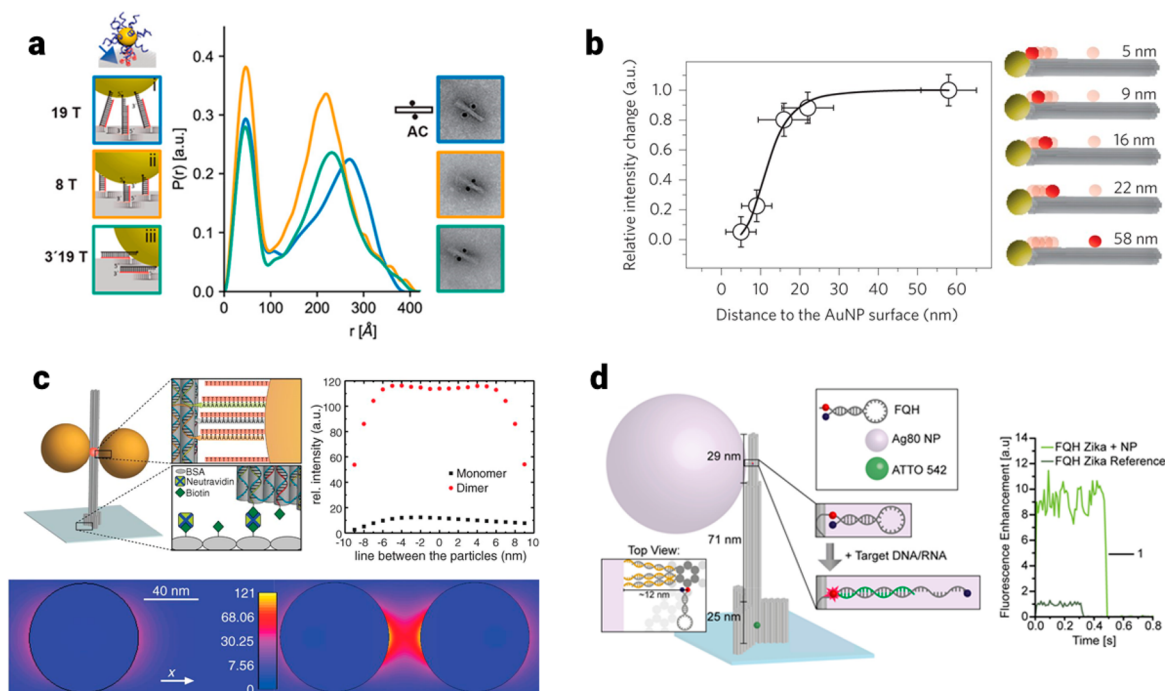


Figure 1. Nanoparticle placement on DNA origami for fluorescence enhancement. (a) (left) Scheme of different connector types: (i) A_{15} to T_{19} (blue), (ii) A_9 to T_8 (orange), and (iii) A_{15} to $3' T_{19}$ (green, zipper configuration). (right) PDDF for each of the three different connector types for dimers shown together with corresponding TEM images.²⁰ (b) Normalized and threshold-corrected fluorescence intensity measurements (circles) of Cy5 dyes at varying distances from a AuNP and the corresponding fit (curve).⁴² (c) (top, left) Sketch of the DAN with two AuNPs forming a dimer, with a dye (red sphere) between the NPs. (top, right) Numerical simulations of the FE for a dye oriented in the radial direction in a plasmonic hot spot. a.u., arbitrary units. (bottom) Numerical simulation of electric field intensity for a monomer (left) and dimer (right).³⁵ (d) (left) DAN with a fluorescence quenching hairpin. (right) FE in a DAN with a AgNP compared to a reference without AgNP.³⁹ (a) Reproduced with permission from ref 20. Copyright 2018 American Chemical Society. (b) Reproduced with permission from ref 42. Copyright 2013 Springer Nature. (c) Reproduced with permission from ref 35. Copyright 2012 The American Association for the Advancement of Science. (d) Reproduced with permission from ref 39. Copyright 2017 American Chemical Society.

hybridization of the two strands, the duplex is oriented perpendicular to the bound surfaces (Figure 1a). For the zipper configuration, the two different terminal ends protrude, which, upon binding, results in a duplex that is oriented tangentially to the bound surfaces. In a study by Hartl et al.²⁰ small-angle X-ray scattering (SAXS) was used to accurately determine the distances between spherical nanoparticles bound to predefined positions on a rectangular DNA origami block in the zipper and the shear configuration with varying lengths of sequences (Figure 1a). Interparticle distances for structures utilizing shear geometry connectors followed an expected trend, with the longer T_{19} connector spacing the particles 5 nm further apart than the T_8 connector, a difference coinciding with the difference in the connector lengths. Notably, the zipper configuration did not yield the smallest interparticle distances. This was explained by the presence of the single-stranded DNA shell around the particles, which sterically hinders the placement of particles close to a surface. The formation and application of complex hybrid structures where both fluorescent dyes and metal nanoparticles are arranged on the same DNA origami structure was shown, for example, by Schreiber et al. (Figure 1b).⁴² By arranging Cy5 dye molecules at varying discrete distances from a central core gold nanoparticle, the authors were able to verify a $1/d^4$ distance dependence model of quenching.

Detection of single molecules with a fluorescence microscope requires sensitive cameras, and the discrimination of

real events from noise can be tedious. A plasmonic enhancement can lower the bar for the complexity of the instrumentation required for the detection of fluorescence events.⁴³ Although ensemble-averaged biosensors for the detection of RNA, DNA, and proteins have depended on plasmon-enhanced fluorescence for years, the advent of DNA origami-based single-molecule sensors relying on plasmon enhancement is a relatively new development. Acuna et al. reported the bottom-up fabrication of DNA-assembled nanoantennas (DANs), which are composed of a DNA nanopillar arranging two AuNPs with a 23 nm gap between them (Figure 1c).³⁵ An ATTO 647N dye molecule was placed in this plasmonic hot spot between the two particles, and the fluorescence properties of the hybrid structure were then probed. The authors reported FE of up to 117-fold for DANs carrying 100 nm particles. This significance of the DANs lies in the deterministically assembled nanoparticle dimers for the signal detection and amplification of individual dye molecules. This work opened up space for numerous studies building on this concept.

One challenge, for example, in molecular diagnostics is the low signal-to-noise ratio in biological samples, since analytes often contain not only the target molecules but also many other species that can contribute to binding interactions and cause spurious detection events. Single-molecule detection, therefore, requires the isolation of the fluorescence signal of the molecule of interest from background contributions by other equivalent molecules or impurities. Additionally, using

diffraction-limited optics to observe single-molecule events restricts detection volumes to the femtoliter range (the space of $1\ \mu\text{m}^3$, which is a lot of space for nanometer-sized molecules) and concentrations to pico- or nanomolar ranges, whereas most biological reactions occur at the micromolar range and on the nanometer scale. Tinnefeld and co-workers overcame these obstacles in a series of works. Puchkova et al. used the DANs described above to achieve a single-molecule detection of ATTO 647N dye molecules at dye concentrations of up to $25\ \mu\text{M}$ in the presence of NiCl_2 acting as a quencher.³⁶ They also achieved an FE of 5468 \times , the highest enhancement factor for a dimer nanoantenna at the time. The FE capacity of an optical nanoantenna is the result of two contributions: the electric-field intensity enhancement at the dye's excitation wavelength and the relative change in the dye's quantum yield induced by the nanoantenna at the dye's emission wavelength range. To optimize these two parameters, the authors controlled distinct characteristics in their nanoantenna system: they used the zipper geometry to reduce the interparticle distance, the dimer orientation and the incident polarization were aligned, and they quenched the intrinsic quantum yield of the fluorophore to measure its effect on the fluorescence enhancement in DANs.

When using gold nanoparticles as the active material species, the FE is restricted to the red–near-infrared (NIR) spectral range. To expand the spectral range and increase the signal strength, various strategies have been pursued. Zhang et al. fabricated gold nanorod dimers on a DNA origami structure to construct DANs, which they then used to study the FE of ATTO 655 dye molecules.⁴⁴ The authors probed the effect of varying gap distances between the nanorod tips on the FE, where the lowest gap distance of 6.1 nm resulted in the highest experimental FE factor of 473, whereas finite-difference time-domain (FDTD) simulations provided a theoretical maximum FE factor of ~ 1200 . Vietz et al. replaced the AuNPs with spherical silver nanoparticles (AgNPs), which show both a lower absorption and higher scattering cross-section over a broader spectral band in the visible range compared to AuNPs.³⁷ The authors measured the FE of three different types of dyes—Alexa 488, ATTO 542, and ATTO 647N—and found that the AgNP DANs resulted in mean FE values of ~ 139 , 149, and 162 for the three dyes, respectively. This established the superior plasmonic performance and broadband FE capabilities of AgNPs compared to the AuNP DANs, which gave FE values of 1.53, 3.07, and 176, respectively. It is worth mentioning that circularly polarized light was employed in the experiments to minimize the dispersion of FE distributions due to the random orientation of the DANs on glass slides. However, this created a challenge when comparing experimental and simulated results, because the dyes were free to rotate on time scales orders of magnitude faster than the acquisition integration time. With the goal to employ their nanoantenna devices as a sensing platform, Vietz et al. then introduced a fluorescence quenching hairpin (FQH) that exhibits a $217 (\pm 31)$ -fold FE for the unquenched dye configuration (corresponding to an open hairpin).³⁸ The authors further designed the hairpin to promote a direct contact between the dye ATTO 647N and the quencher BBQ650, leading to the formation of ground-state complexes that exhibit a negligible radiative rate. Notably, this nanoantenna utilized only a single AgNP, as the presence of the hairpin sterically hindered the attachment of a second particle.

In the next step, the same group used the AgNP DAN in combination with FQH for a single-molecule detection of a synthetic Zika virus-specific sequence in a buffer as well as human blood serum (Figure 1d).³⁹ Kaminska et al. then used DANs for the FE of a single peridinin–chlorophyll *a*–protein complex, a light-harvesting complex, placed in the plasmonic hot spot of both Ag and AuNP dimer antennas.⁴⁰ Although there had been previous reports on the plasmonic enhancement of light-harvesting complexes,^{45,46} further development was hindered by the lack of a technique for their precise placement inside hot spots. The AuNP and AgNP nanoantennas resulted in FEs of up to 526-fold and 250-fold, respectively. Interestingly, the DANs show a considerable dispersion in both fluorescence intensity and fluorescence lifetime. Possible reasons for this include the occasional formation of monomer antennas along with dimer antennas, as well as inhomogeneities in the NP shape and size as well as variable interparticle gap sizes. Recently, Trofymchuk et al. developed a new DNA origami design that features a “window” in the hot spot of the DANs.⁴¹ The rationale of this design change is to expand the space and reduce the influence of steric effects on the binding of incoming target molecules to ligands positioned in the hot spot. The new design yielded equivalent and higher values of FE (up to 417 \times) of ATTO 647N dye molecules. The authors then placed a sandwich binding assay for the detection of a DNA fragment specific to Oxa-48, an enzyme providing resistance to a certain antibiotic. This type of test is used for the diagnosis of *Klebsiella pneumoniae* infections. By positioning three capture strands in the hot spots, FE values of up to 461 \times could be achieved. Again, the FE distribution exhibits a broad distribution, attributed to the effects mentioned above. Along with this, comparatively low binding efficiencies of 66% (with AgNPs) compared to 84% (for reference structures without AgNPs) might also limit the degree of the FE. Nevertheless, an impressive achievement of the work is the successful use of a smartphone camera for a single-molecule detection using the DANs. Integrating these components into a simple microscope setup, the observation of single-molecule blinking and bleaching events was possible with off-the-shelf consumer products.

■ SERS SENSORS BASED ON DNA ORIGAMI

Surface-enhanced Raman spectroscopy (SERS) is a surface-specific spectroscopic technique that employs metal surfaces to enhance Raman signals of molecules. Next to rugged metal surfaces, metal nanoparticles are routinely used in a SERS application. During the interaction of light with the plasmonic nanoparticles, oscillations of the electron plasma are excited on the metallic surfaces leading to an enhancement of the electric field in close vicinity to the particles and, hence, to an amplification of the molecular Raman signal.⁴⁷ Importantly, the intensity of the electric field is not evenly distributed around the nanoparticles, but hot spots emerge where nanoparticles come close together or nanoparticles exhibit spikes or tips.⁴⁸ In such regions, the Raman scattering intensity is extremely enhanced, as the Raman signal grows with the fourth power of the electric field. Hence, signal boosts up to 15 orders of magnitude in comparison with nonenhanced Raman scattering can be achieved.⁴⁸ Because of the huge signal enhancement provided by plasmonic hot spots, SERS can become a highly sensitive spectroscopic method and provide the means for single-molecule studies.⁴⁹

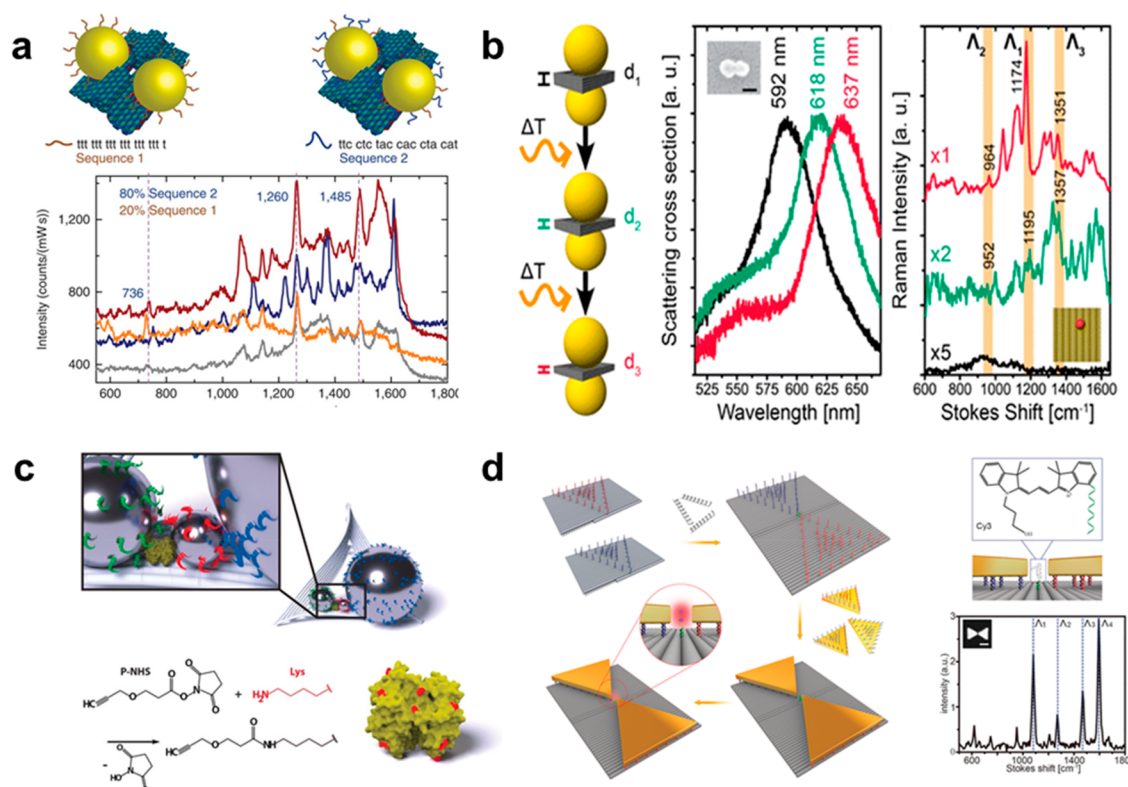


Figure 2. DNA origami-based SERS nanoantennas. (a) Plasmonic dimers of gold spheres covered with two different DNA sequences. (below) Their SERS spectra.⁵² (b) Thermally induced hot-spot shrinkage and corresponding scattering (middle) and Raman (right) spectra with different gap size.⁵⁵ (c) Single streptavidin molecule immobilized in the hot spot of silver nanolenses.⁵⁶ (d) Schematic representation of the synthesis of a gold bowtie nanoantenna (left) and Raman spectrum of single Cy3 molecule (right).⁵⁷ (a) Reproduced with permission from ref 52. Copyright 2014 Springer Nature. (b) Reproduced with permission from ref 55. Copyright 2016 American Chemical Society. (c) Reproduced with permission from ref 56. Copyright 2018 Wiley-VCH. (d) Reproduced with permission from ref 57. Copyright 2018 Wiley-VCH.

It is thus crucial to find precise and reliable ways for the fabrication of versatile hot-spot-based SERS sensors. The first requirement for such a sensor is the accurate arrangement of plasmonic nanoparticles with small interparticle gaps of ~ 5 nm or below. Second, the molecule of interest must be precisely placed in the hot spot to provide a strong and targeted Raman signal. These conditions are hard to fulfill using conventional top-down fabrication methods such as electron-beam lithography. Thanks to its addressability, specificity, and nanometer precision, DNA molecules, along with DNA origami structures, become natural candidates for the fabrication of versatile Raman-active antenna structures. The standout example of such structures is the synthesis of nanogap core-shell gold particles presented by Lim et al. In their approach the synthesis of the homogeneous Raman-active gap of 1 nm between the core and the shell was facilitated by DNA molecules on the core's surface, which enabled the detection of single molecules placed in the gap.⁵⁰ A pioneering study using DNA origami in SERS was performed by Prinz et al. in 2013.⁵¹ They used two spherical gold nanoparticles attached to a triangular DNA origami to obtain Raman spectra of molecules embedded in the DNA structure. Shortly after, Thacker et al. used a more sophisticated DNA origami design for binding spherical gold nanoparticles with a predetermined sub-5 nm gap. The synthesized structures were used for Raman measurements of Rhodamine 6G and DNA enveloping nanoparticles (Figure 2a).⁵² At the same time, Kühler et al. observed Raman spectra of SYBR-Gold molecules that accumulated in the designed

gap of a DNA origami-gold nanoparticle hybrid structure.⁵³ For single-molecule measurements, further shrinkage of the interparticle gap had to be realized, which was achieved by two different approaches.^{54,55} The first approach was based on the overgrowth of a silver shell on gold nanoparticles attached to DNA origami,⁵⁴ while the second approach utilized a thermally induced shrinkage of the DNA origami structure to which the gold particles were anchored (Figure 2b).⁵⁵

Significant effort has been put into developing DNA sensors with novel plasmonic properties and enhanced sensitivity, obtained often via the synthesis of plasmonic arrays.^{56,58–62} One possible fabrication methodology of nanoantenna arrangements is a “polymerization” of monomeric DNA origami units into long chains or two-dimensional (2D) lattices using complementary strand hybridization.^{58,59} The most straightforward realization of this concept was reported by Zhao et al., where long plasmonic chains were obtained by linking rectangular DNA origamis, each containing two 30 nm gold nanoparticles.⁵⁸ An enhanced Raman signal of mercaptobenzoic acid (MBA) molecules was explained by the formation of multiple hot spots, a result of the chain formation. Furthermore, because of its programmability, DNA nanotechnology enables the synthesis of more sophisticated plasmonic systems. For example, Ag@Au core-shell nanoparticles were arranged into a series of hexagonal clusters using DNA origami and then used for the detection of MBA molecules.⁶⁰ Another interesting refinement of DNA origami-based sensors was presented by Moeinian et al.⁶¹ In their approach, a silicon nanowire was functionalized with nano-

particle-decorated 6-helix bundles to realize a sub-wavelength spatial precision of SERS measurements. Despite the significant advantages of plasmonic sensors, many of them rely on the random deposition of molecules on the surface of plasmonic particles for SERS measurements and hence do not utilize virtues of DNA origami, namely, programmability and nanometer precision. A “quantized” molecular sensor using DNA origami multimers with precisely localized dye molecules was reported by Fang et al.⁶² Because of finely organized large gold nanoparticles, a plasmonic coupling between nanoparticles was achieved. The calculated enhancement factor was on the order of 10^8 , which enabled the detection of a single carboxy-X-rhodamine molecule anchored in the hot-spot region. Recently, DNA origami has also been applied to precisely accommodate a single protein in the hot spot of silver nanolenses.⁵⁶ Subsequently, the plasmonic nanoparticles’ arrangement enabled measurements of a single molecule of alkyne-functionalized Streptavidin, indicating future applications of DNA origami-based nanoantennas in biosensing (Figure 2c).

Thus, DNA origami-based nanoantennas have already helped to strongly increase the sensing utility of Raman spectroscopy. This was mainly realized by shrinking the gap sizes, by multiplication of hot-spots, or by the growth of silver layers on the antenna particles. However, the plasmonic properties of such antenna systems can be tuned further. For example, anisotropic nanoparticles with sharp edges can be integrated into DNA origami SERS sensors. Anisotropic nanostructures display exquisite plasmonic properties due to the tremendous field enhancement at their tips.⁶³ Moreover, the use of anisotropic nanoparticles allows a convenient tuning of plasmonic properties, which are strongly correlated with particle shape and size.^{48,63} Despite these advances, to our knowledge, only two DNA origami sensors utilizing anisotropic nanoparticles have been reported.^{57,64} Tanwar et al. reported the synthesis of gold nanostar dimers and their use in the single-molecule measurement of Texas Red, a fluorescent dye.⁶⁴ Coupling between the sharp tips of the nanoparticles contributed to very strong signal enhancement, up to 8×10^9 , in the hot spot between nanostars. A similar signal enhancement was recently obtained by the tip-to-tip arrangement of two gold nanolenses on DNA origami, enabling the detection of single Cy3 and Cy5 molecules (Figure 2d).⁵⁷

■ DNA ORIGAMI-BASED CHIRAL PLASMONIC SENSING

Another promising route toward the development of biosensing platforms is the use of chiroptical properties of plasmonic nanostructures or the plasmon-enhanced detection of chiral molecules.^{65,66} For this, circular dichroism (CD) spectroscopy is employed to analyze the chirality of the structures by measuring the difference in the absorption of left-handed (LH) and right-handed (RH) circularly polarized light. Most of the biomolecules such as DNA and proteins typically exhibit CD signals in the ultraviolet range.⁶⁷ In contrast to biomolecules, chiral plasmonic systems display strong and characteristic CD responses in the visible regime due to the surface plasmon resonances.^{68–70} This makes chiral plasmonic devices ideal for the detection of biomolecules in solution, since many biological samples show a very low “background” CD signal in the visible range. Surface plasmons of colloidal metal nanoparticle assemblies can significantly

enhance the CD signals⁷¹ and thus enable the detection of biomolecules in the visible wavelengths with increased sensitivity.⁷²

By leveraging the programmability and scalability of DNA self-assembly, colloidal nanoparticles have been self-assembled into LH or RH plasmonic helical structures,^{69,73} pyramids,⁷⁴ tetramers,⁷⁵ toroidal superstructures,⁷⁶ or helical superstructures.^{77,78} Such static chiral assemblies show strong plasmon-mediated CD responses. However, for sensing applications dynamic chiral plasmonic structures proved to be more viable thus far.⁶ Among various dynamic chiral plasmonic assemblies,^{70,79,80} the reconfigurable three-dimensional (3D) plasmonic metamolecules introduced by Kuzyk et al.⁸¹ have been particularly successful as sensing devices. This chiral metamolecule is composed of two linked DNA origami bundles each hosting a gold nanorod at the top and bottom, forming a 3D plasmonic cross structure (Figure 3a). The relative angle between the rods and therefore the chiral state of the device can be modulated by DNA-, RNA-, or aptamer-based locks, which are extended from the edges of the DNA origami bundles. With an addition of specifically designed DNA fuel strands or with a target molecule binding, the sensing devices switch their conformation from an “open” or “relaxed” achiral state to one of the “locked” chiral states (LH or RH). These structural configurations can be correlated with the corresponding optical responses using CD spectroscopy in real time.

By using the original plasmonic metamolecule or similar chiral plasmonic structures, this versatile approach was extended to stimuli including light,^{82–84} pH,^{84–86} temperature,⁸⁷ small molecules,^{87,88} proteins,⁸⁹ DNA,^{81,90} and viral RNA.⁹¹ Figure 3a,b shows examples of DNA origami-based switchable chiral plasmonic biosensors for the detection of various analytes. Our research group demonstrated a selective detection of viral RNA from the hepatitis C virus genome at target concentrations of below 100 pM in buffer⁹¹ (Figure 3a). For the biorecognition, two complementary locking DNA strands are extended from the DNA origami bundles, and the hybridization of these two strands to each other is prevented by a third strand that is complementary and therefore bound to one of the two locking strands. This blocking strand is removed by the target RNA sequence by a toehold-mediated strand displacement. After this removal step, the two locking DNA strands are now free to hybridize to each other leading to the formation of the RH state of the device with a distinct optical response measured by CD spectroscopy (Figure 3a). We further proved that our sensors are still stable and functional after 30 min of incubation in 10% human blood serum and can detect the target RNA at concentrations below 1 nM in 10% serum. This sensing device can readily be applied to detect RNA from the SARS-Cov-2 (to be published).

In 2018, Zhou et al. reported a dual responsive plasmonic sensing device that can respond to temperature and aptamer-target interactions.⁸⁷ The versatility and addressability of DNA origami enabled the detection of adenosine triphosphate (ATP) and cocaine (COC) molecules in a single device by jointly introducing split ATP and COC aptamers to the DNA origami structure. Chiroptical responses of this reversible sensing device in the presence of target ATP (1 mM) and COC (1 mM) molecules could be monitored by CD spectroscopy. As shown by the black curve in the CD spectra in Figure 3b, without target binding the device displays slight

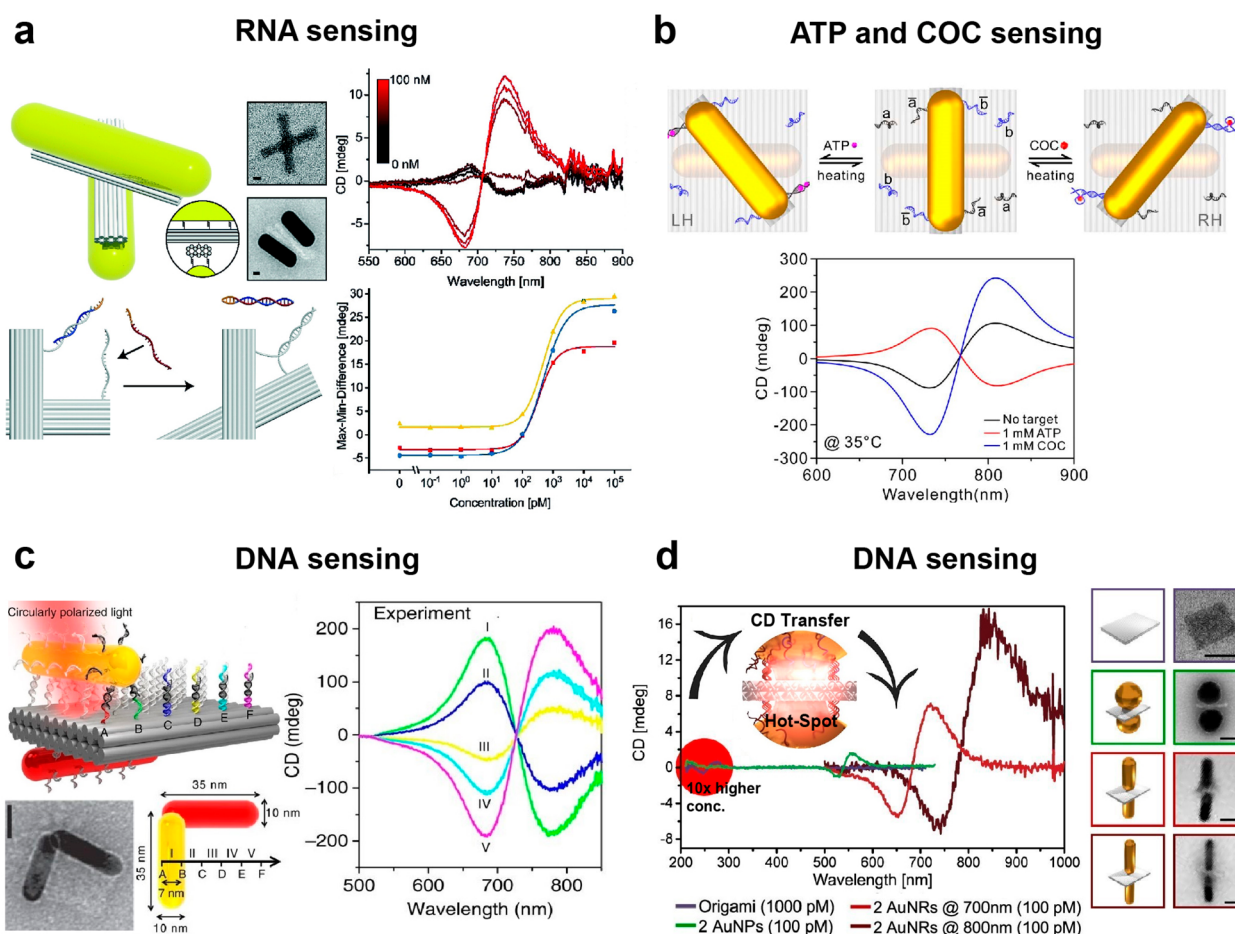


Figure 3. DNA origami-enabled chiral plasmonic sensing systems. DNA origami-based switchable chiral plasmonic biosensors for detection of viral RNA (a), ATP, and COC (b), and their corresponding CD responses at different target concentrations. Chiral plasmonic walker assembled on DNA origami and measured CD spectra at different stations, potentially acting as nucleic acid sensor (c). DNA origami-supported nanoantennas for the detection of chiral B-form DNA molecules and CD measurements of nanoantennas in solution (d). Schematics and TEM micrographs (in a, c, d) of assembled sensing devices, scale bars are 20 nm (in a, c) and 40 nm (in d). (a) Reproduced with permission from ref 91. Copyright 2018 Wiley-VCH. (b) Reproduced with permission from ref 87. Copyright 2018 American Chemical Society. (c) Reproduced with permission from ref 90. Copyright 2015 The Authors. (d) Reproduced with permission from ref 72. Copyright 2018 American Chemical Society.

signatures of the RH state. After addition of the ATP molecules, the CD spectra flipped (red curve), indicating that the device switched into the LH state. Contrarily, when COC molecules were added, the device was driven further into the RH state reflected in stronger CD responses (blue curve). The authors also showed in this study that the chiral state of the device can be tuned by temperature. Using a similar geometry, Dong et al. recently reported DNA origami-based adaptive plasmonic logic gates that read multiple DNA molecules as input and return plasmonic chiroptical signals as output.⁹² Such self-assembled systems perform logical computations and could also work as plasmonic sensors. Similarly, Huang et al. demonstrated a reconfigurable chiral plasmonic sensor where “double-stranded” and “split aptamer” locks are employed as biorecognition elements for adenosine sensing.⁸⁸ They tested different lock systems at different adenosine concentrations and achieved the detection limit of 20 μM with a response time of 1 min. They found that shortening the hybridization length of the locks is crucial to improve the detection limit and response time. Subsequently, Funck et al. reported a dual-aptamer-functionalized sensing device that could reliably detect the human α -thrombin protein in solution with a detection limit of 100 pM.⁸⁹ This device could potentially be

further improved by introducing multiple copies of the thrombin aptamers to the DNA origami structures.

Next, Zhou et al.⁹⁰ demonstrated a chiral plasmonic walker system that, in principle, can be used as a sensor to detect a target nucleic acid sequence. As shown in Figure 3c, the chiral plasmonic walking system formed by assembling a walker AuNR (yellow) and a stator AuNR (red) in a chiral geometry on two opposite faces of a DNA origami structure. After the sequential addition of respective blocking and removal strands, the walker performs a progressive and directional movement with a “rolling” fashion. The overall walking process was in situ optically monitored with an immediate spectral response by CD spectroscopy (Figure 3c, CD spectra). This approach was further advanced by introducing a walker couple that performs independent or simultaneous stepwise walking along the same track,⁹³ a rotary plasmonic nanoclock that can perform a directional and reversible 360° rotation,⁹⁴ and a sliding system that can slide two DNA origami filaments using gold nanoparticles.⁹⁵ Remarkably, these dynamic plasmonic systems could resolve the stepwise movement with nanoscale step size, which is far below the optical diffraction limit.

Thus far, we have reviewed DNA origami-templated reconfigurable chiral plasmonic sensing devices. Alternatively,

there is another approach to use DNA origami-based static plasmonic nanostructures for the detection of chiral biomolecules. This approach is based on an enhanced CD spectroscopy and an ultrasensitive detection of (chiral) molecules by surface plasmon-generated near-fields.^{96–100}

Figure 3d shows an example of DNA origami-supported nanoantennas for the detection of a B-form DNA chirality.⁷² In this report, our research group demonstrated that the UV-CD response of DNA molecules can be transferred into the resonance frequency range of plasmonic nanoantennas. The high electromagnetic field enhancement in the antenna hot spot allowed detection of the transferred CD signal at much lower analyte concentrations than the amount needed to obtain discernible CD signals from the pristine DNA molecules in the UV. Figure 3d shows the experimental design and the transfer of the UV-CD signal of a two-layered DNA origami sheet to the visible regime and its amplification by a factor of 30 with the help of two spherical AuNPs (green curve). By using AuNRs antenna structures, the CD transfer into the near-infrared regime is realized with an up to 300-fold stronger CD signal (red and dark red curves). We also showed that the use of other materials (gold–silver, core–shell particles) for the antenna element enables the shifting of the CD signal into yet another wavelength range.

■ CONCLUSION AND GENERAL PERSPECTIVES

In the past decade, the DNA origami-based fabrication of plasmonic sensors has advanced rapidly.^{101–104} In summary, DNA origami is a successful nanofabrication technology to arrange plasmonic nanoparticles with nanometer precision.^{69,105–109}

Specificity and sensitivity are key variables when describing the performance of a sensor. To study these parameters and to increase performances of sensors, DNA origami provides the molecular breadboard for well-defined interactions of target molecules with the recognition elements.

The addressability of DNA origami allows, for example, the accurate positioning of fluorescent markers in the plasmonic hot spot of nanoparticle antennas, and this has been used to achieve a single-molecule sensing of a variety of targets. Currently, when studying FE-based sensing, spherical nanoparticles have received the greatest attention, while nanorods have been explored to a lesser extent. This highlights an area of interest with a high potential that has remained relatively unexplored, as anisotropic morphologies like nanorods as well as more exotic structures such as bipyramids are known to have higher field-intensity increases at their tips.¹¹⁰ This property could lead to a further enhancement in the sensitivity of such sensors. An interesting development is the use of an off-the-shelf consumer smartphone to readout the fluorescence signals from DNA-assembled antennas. This line of research could be extended to increase both the limit of detection from such instruments as well as the range of analytes that can be detected potentially enabling pathogen detection in remote areas.

The ability to arrange plasmonic nanoparticles on DNA origami also renders it an exquisite platform for the fabrication of plasmonic SERS sensors, especially for single-molecule measurements. Moreover, DNA nanostructures are fully biocompatible and can be readily functionalized with a variety of targeting entities including aptamers and antibodies.^{111–114} Nevertheless, up to now, DNA origami-based SERS sensors were primarily used for the detection of small dyes, with only

one functional biomolecule measurement reported.⁵⁶ Hence, future efforts in the field should be focused on the enhancement of sensitivity and versatility of such SERS sensors and their use in studies of various biomolecules both in vitro and in situ.

The combination of chiral plasmonics and DNA origami has enabled chirality-based biosensors for the selective and sensitive detection of various analytes. For a wide range of detection windows (UV–vis–NIR), the optical responses can be tuned and amplified by size, shape, and material composition of plasmonic building blocks. For example, recently we demonstrated that chiral assemblies of gold–silver core–shell plasmonic nanorods show strongly increased CD responses compared to their gold counterparts.¹¹⁵ Furthermore, by controlling the size, aspect ratio, and silver shell thickness, the spectral responses could be tuned as desired. This could dramatically improve the performance of the aforementioned devices. In addition, programmable and fully addressable DNA origami enables incorporating multiple biorecognition elements. This opens numerous sensing systems that respond to various molecular binding events, facilitating the detection of a wide variety of molecular targets with a high specificity and selectivity. Recently, “single-structure” CD measurements were shown without DNA origami in plasmonic nanorod dimers assembled with the help of bovine serum albumin (BSA).¹¹⁶ On the one hand, it will be of outstanding interest to study a single-structure CD in a well-controlled DNA origami nanofabrication scheme. On the other end, a naked-eye detection of chiral structures is possible with a simple configuration of two crossed polarizers.⁶⁹ This could, at some point, enable a sensitive pathogen detection without the need for expensive equipment. Thus, the overall concept of chirality-based detection holds great potential for the further development of plasmonic biosensing.

DNA origami-based plasmonic sensors are fabricated in an aqueous solution and are therefore, in principle, suited for sensing applications inside cells and tissues. Such plasmonic probes could be applied to study, for example, single-molecule processes on cell surfaces. Nevertheless, because of the reduced stability of DNA origami-assembled plasmonic nanostructures in in vivo conditions, real-life sensing applications are challenging and will require more in-depth research. Besides natural cells, these probes can be integrated into more defined synthetic biology systems, for example, synthetic cells. One example could be chiral plasmonic walkers that sense their biochemical surroundings, transport cargo in synthetic cells, and report their status optically in real-time.

To achieve a more widespread adoption of DNA origami-based plasmonic sensors, it is crucial to apply these sensors without specialized and expensive equipment such as CD spectrometers or single-molecule fluorescence setups. Improvements in DNA origami nanofabrication will enable stronger signals. In consequence, this enables optical readouts with as little instrumentation as a smartphone or a standard optical microscope with built-in polarizers.¹¹⁷ This will bring the benefits of DNA origami-assembled plasmonic nano-devices to researchers of various fields, from cell biology to medical diagnostics and optics. Interestingly, custom-made DNA origami nanostructures assembled with fluorophores and nanoparticles are already commercially available (tilbit GmbH, gattaquant GmbH).

One factor that has limited the application of DNA origami structures is their reduced stability in the presence of DNA

nucleases, at low salt concentrations, at elevated temperatures, and at varying pH values. In recent years, a variety of stabilization strategies have been developed. Examples include coating layers with polymers,^{118–120} silica,¹²¹ peptoids,¹²² as well as cross-linking,^{123,124} among others. In the next years, it will be important to study the performance of stabilized DNA origami-assembled plasmonic sensors in application-oriented settings, for example, in blood.

With increasing knowledge about the fabrication of DNA origami-based plasmonic nanostructures, larger 3D structures can be built.^{125–128} Mastering the complex assembly processes of, for example, lattices would enable the self-assembly of photonic crystals with tailored photonic band gaps that could be integrated into optical circuitry or deposited on surfaces. At the same time, many commercial applications are not profitable due to the high price of DNA. Because of advances in the production of DNA, costs are falling rapidly. With this, DNA origami-based sensors become economically viable. A biological mass production of DNA in bioreactors enables prices of 200 € per gram. This equals to $\sim 10^{17}$ DNA origami-assembled plasmonic sensors.¹²⁹

In conclusion, the DNA origami-based fabrication of plasmonic sensors is a new technological platform to engineer sensors with great control over dimensions and the very building blocks on the molecular scale. DNA origami-assembled plasmonic sensors thus probably have reached a level of technological maturity that enables their application in real-world settings.

AUTHOR INFORMATION

Corresponding Author

Tim Liedl – Faculty of Physics and Center for NanoScience, Ludwig-Maximilians-University, 80539 Munich, Germany; orcid.org/0000-0002-0040-0173; Email: tim.liedl@physik.lmu.de

Authors

Mihir Dass – Faculty of Physics and Center for NanoScience, Ludwig-Maximilians-University, 80539 Munich, Germany

Fatih N. Gür – Faculty of Physics and Center for NanoScience, Ludwig-Maximilians-University, 80539 Munich, Germany

Karol Kołataj – Faculty of Physics and Center for NanoScience, Ludwig-Maximilians-University, 80539 Munich, Germany

Maximilian J. Urban – Faculty of Physics and Center for NanoScience, Ludwig-Maximilians-University, 80539 Munich, Germany

Complete contact information is available at: <https://pubs.acs.org/10.1021/acs.jpcc.0c11238>

Author Contributions

The manuscript was written through the contributions of all authors. All authors have given approval to the final version of the manuscript.

Notes

The authors declare no competing financial interest.

Biographies



Mihir Dass is currently a Marie Skłodowska-Curie doctoral fellow in the group of Prof. Tim Liedl at LMU, Munich. He received his Bachelor's and Master's degree in Nanotechnology (2017) from Amity University, India. His research interests include dynamic DNA nanotechnology, plasmonics, and nanofabrication.



Fatih N. Gür is currently a postdoctoral fellow in the group of Prof. Tim Liedl, LMU Munich. He received his B.Sc. degree (2010) in Physics from Izmir Institute of Technology, Turkey, M.Sc. degree (2012) in Nanoscience and Nanotechnology from KU Leuven, Belgium, and Ph.D. degree (2018) in Physical Chemistry from the Center for Advancing Electronics Dresden, TU Dresden, Germany. His research interests lie in the field of DNA nanotechnology including DNA-assembled plasmonic nanostructures, dynamic DNA nanodevices, and their applications.



Karol Kołataj is currently a Marie Skłodowska-Curie fellow and a postdoc in the group of Prof. Tim Liedl, LMU Munich. He received his B.Sc. degree (2012) in Biotechnology from Warsaw University of

Life Sciences and his M.Sc. degree (2014) in Chemistry and Ph.D. degree in Physical Chemistry from the University of Warsaw. His areas of expertise include the fabrication of plasmonic nanoparticles, DNA nanotechnology, and surface-enhanced Raman spectroscopy.



Maximilian J. Urban is currently a postdoctoral fellow in the group of Prof. Tim Liedl, LMU Munich. He received his B.Sc. and M.Sc. (2014) degrees in Life Science from the Universität Konstanz, Germany, and his Ph.D. degree in Physical Chemistry from the Universität Heidelberg and the Max Planck Institute for intelligent Systems, Stuttgart, Germany. His research interest is the application of DNA nanotechnology and plasmonics for sensing.



Tim Liedl is professor for experimental physics at LMU. He received his diploma in physics in 2004 in the group of Wolfgang J. Parak, where he worked on the development of hydrophilic coatings for fluorescent semiconductor nanoparticles. In 2007 he obtained his Ph.D. in the group of Friedrich C. Simmel studying DNA-based nanodevices and switches, which are driven by chemical oscillations. From 2007 to 2009 he visited William M. Shih's laboratory at the Dana-Farber Cancer Institute/Harvard Medical School, where he used the DNA-origami method to construct self-assembling two- and three-dimensional structures. The research of Tim Liedl currently focuses on the application of DNA-based nanostructures in biophysics and for self-assembled plasmonic materials.

ACKNOWLEDGMENTS

M.D. and K.K. have received funding from the European Union's Horizon 2020 research and innovation program under the Marie Skłodowska-Curie Grant No. 765703. T.L., F.N.G., and M. J. U. acknowledge funding from the ERC consolidator grant "DNA functional lattices" (Project ID: 818635).

REFERENCES

- (1) Stewart, M. E.; Anderton, C. R.; Thompson, L. B.; Maria, J.; Gray, S. K.; Rogers, J. A.; Nuzzo, R. G. Nanostructured Plasmonic Sensors. *Chem. Rev.* **2008**, *108* (2), 494–521.
- (2) Homola, J. Surface Plasmon Resonance Sensors for Detection of Chemical and Biological Species. *Chem. Rev.* **2008**, *108* (2), 462–493.
- (3) Li, M.; Cushing, S. K.; Wu, N. Plasmon-Enhanced Optical Sensors: A Review. *Analyst* **2015**, *140* (2), 386–406.
- (4) Smith, D. M.; Keller, A. DNA Nanostructures in the Fight Against Infectious Diseases. *Adv. NanoBiomed Res.* **2021**, 2000049.
- (5) Shen, B.; Kostianen, M. A.; Linko, V. DNA Origami Nanophotonics and Plasmonics at Interfaces. *Langmuir* **2018**, *34* (49), 14911–14920.
- (6) Loretan, M.; Domljanovic, I.; Lakatos, M.; Rüegg, C.; Acuna, G. P. DNA Origami as Emerging Technology for the Engineering of Fluorescent and Plasmonic-Based Biosensors. *Materials* **2020**, *13* (9), 2185.
- (7) Holliday, R. A Mechanism for Gene Conversion in Fungi. *Genet. Res.* **1964**, *5* (2), 282–304.
- (8) Kallenbach, N. R.; Ma, R.-I.; Seeman, N. C. An Immobile Nucleic Acid Junction Constructed from Oligonucleotides. *Nature* **1983**, *305* (5937), 829–831.
- (9) Seeman, N. C. Nucleic Acid Junctions and Lattices. *J. Theor. Biol.* **1982**, *99* (2), 237–247.
- (10) Seeman, N. C. DNA in a Material World. *Nature* **2003**, *421* (6921), 427–431.
- (11) Winfree, E.; Liu, F.; Wenzler, L. A.; Seeman, N. C. Design and Self-Assembly of Two-Dimensional DNA Crystals. *Nature* **1998**, *394* (6693), 539–544.
- (12) Ke, Y.; Ong, L. L.; Shih, W. M.; Yin, P. Three-Dimensional Structures Self-Assembled from DNA Bricks. *Science* **2012**, *338* (6111), 1177–1183.
- (13) Hong, F.; Jiang, S.; Lan, X.; Narayanan, R. P.; Šulc, P.; Zhang, F.; Liu, Y.; Yan, H. Layered-Crossover Tiles with Precisely Tunable Angles for 2D and 3D DNA Crystal Engineering. *J. Am. Chem. Soc.* **2018**, *140* (44), 14670–14676.
- (14) Shih, W. M.; Quispe, J. D.; Joyce, G. F. A 1.7-Kilobase Single-Stranded DNA That Folds into a Nanoscale Octahedron. *Nature* **2004**, *427* (6975), 618–621.
- (15) Rothmund, P. W. K. Folding DNA to Create Nanoscale Shapes and Patterns. *Nature* **2006**, *440* (7082), 297–302.
- (16) Douglas, S. M.; Dietz, H.; Liedl, T.; Högberg, B.; Graf, F.; Shih, W. M. Self-Assembly of DNA into Nanoscale Three-Dimensional Shapes. *Nature* **2009**, *459* (7245), 414–418.
- (17) Andersen, E. S.; Dong, M.; Nielsen, M. M.; Jahn, K.; Subramani, R.; Mamdouh, W.; Golas, M. M.; Sander, B.; Stark, H.; Oliveira, C. L. P.; et al. Self-Assembly of a Nanoscale DNA Box with a Controllable Lid. *Nature* **2009**, *459* (7243), 73–76.
- (18) Kopperger, E.; List, J.; Madhira, S.; Rothfischer, F.; Lamb, D. C.; Simmel, F. C. A Self-Assembled Nanoscale Robotic Arm Controlled by Electric Fields. *Science* **2018**, *359* (6373), 296–301.
- (19) Funke, J. J.; Dietz, H. Placing Molecules with Bohr Radius Resolution Using DNA Origami. *Nat. Nanotechnol.* **2016**, *11* (1), 47–52.
- (20) Hartl, C.; Frank, K.; Amenitsch, H.; Fischer, S.; Liedl, T.; Nickel, B. Position Accuracy of Gold Nanoparticles on DNA Origami Structures Studied with Small-Angle X-Ray Scattering. *Nano Lett.* **2018**, *18* (4), 2609–2615.
- (21) Mirkin, C. A.; Letsinger, R. L.; Mucic, R. C.; Storhoff, J. J. A DNA-Based Method for Rationally Assembling Nanoparticles into Macroscopic Materials. *Nature* **1996**, *382* (6592), 607–609.
- (22) Alivisatos, A. P.; Johnsson, K. P.; Peng, X.; Wilson, T. E.; Loweth, C. J.; Bruchez, M. P.; Schultz, P. G. Organization of "nanocrystal Molecules" Using DNA. *Nature* **1996**, *382* (6592), 609–611.
- (23) Liu, J.; Lu, Y. Preparation of Aptamer-Linked Gold Nanoparticle Purple Aggregates for Colorimetric Sensing of Analytes. *Nat. Protoc.* **2006**, *1* (1), 246–252.

- (24) Cutler, J. I.; Auyeung, E.; Mirkin, C. A. Spherical Nucleic Acids. *J. Am. Chem. Soc.* **2012**, *134* (3), 1376–1391.
- (25) Liu, B.; Liu, J. Methods for Preparing DNA-Functionalized Gold Nanoparticles, a Key Reagent of Bioanalytical Chemistry. *Anal. Methods* **2017**, *9* (18), 2633–2643.
- (26) Gür, F. N.; Schwarz, F. W.; Ye, J.; Diez, S.; Schmidt, T. L. Toward Self-Assembled Plasmonic Devices: High-Yield Arrangement of Gold Nanoparticles on DNA Origami Templates. *ACS Nano* **2016**, *10* (5), 5374–5382.
- (27) Liu, B.; Liu, J. Freezing-Driven DNA Adsorption on Gold Nanoparticles: Tolerating Extremely Low Salt Concentration but Requiring High DNA Concentration. *Langmuir* **2019**, *35* (19), 6476–6482.
- (28) Liu, B.; Wu, T.; Huang, Z.; Liu, Y.; Liu, J. Freezing-Directed Stretching and Alignment of DNA Oligonucleotides. *Angew. Chem.* **2019**, *131* (7), 2131–2135.
- (29) Liu, B.; Liu, J. Interface-Driven Hybrid Materials Based on DNA-Functionalized Gold Nanoparticles. *Matter* **2019**, *1* (4), 825–847.
- (30) Dulkeith, E.; Morteaux, A. C.; Niedereichholz, T.; Klar, T. A.; Feldmann, J.; Levi, S. A.; van Veggel, F. C. J. M.; Reinhoudt, D. N.; Möller, M.; Gittins, D. I. Fluorescence Quenching of Dye Molecules near Gold Nanoparticles: Radiative and Nonradiative Effects. *Phys. Rev. Lett.* **2002**, *89* (20), 203002.
- (31) Coronado, E. A.; Encina, E. R.; Stefani, F. D. Optical Properties of Metallic Nanoparticles: Manipulating Light, Heat and Forces at the Nanoscale. *Nanoscale* **2011**, *3* (10), 4042–4059.
- (32) Anger, P.; Bharadwaj, P.; Novotny, L. Enhancement and Quenching of Single-Molecule Fluorescence. *Phys. Rev. Lett.* **2006**, *96* (11), 113002.
- (33) Giannini, V.; Fernández-Domínguez, A. I.; Heck, S. C.; Maier, S. A. Plasmonic Nanoantennas: Fundamentals and Their Use in Controlling the Radiative Properties of Nanoemitters. *Chem. Rev.* **2011**, *111* (6), 3888–3912.
- (34) Acuna, G. P.; Bucher, M.; Stein, I. H.; Steinhauer, C.; Kuzyk, A.; Holzmeister, P.; Schreiber, R.; Moroz, A.; Stefani, F. D.; Liedl, T.; et al. Distance Dependence of Single-Fluorophore Quenching by Gold Nanoparticles Studied on DNA Origami. *ACS Nano* **2012**, *6* (4), 3189–3195.
- (35) Acuna, G. P.; Möller, F. M.; Holzmeister, P.; Beater, S.; Lalkens, B.; Tinnefeld, P. Fluorescence Enhancement at Docking Sites of DNA-Directed Self-Assembled Nanoantennas. *Science* **2012**, *338* (6106), 506–510.
- (36) Puchkova, A.; Vietz, C.; Pibiri, E.; Wünsch, B.; Sanz Paz, M.; Acuna, G. P.; Tinnefeld, P. DNA Origami Nanoantennas with over 5000-Fold Fluorescence Enhancement and Single-Molecule Detection at 25 M. *Nano Lett.* **2015**, *15* (12), 8354–8359.
- (37) Vietz, C.; Kaminska, I.; Sanz Paz, M.; Tinnefeld, P.; Acuna, G. P. Broadband Fluorescence Enhancement with Self-Assembled Silver Nanoparticle Optical Antennas. *ACS Nano* **2017**, *11* (5), 4969–4975.
- (38) Vietz, C.; Lalkens, B.; Acuna, G. P.; Tinnefeld, P. Synergistic Combination of Unquenching and Plasmonic Fluorescence Enhancement in Fluorogenic Nucleic Acid Hybridization Probes. *Nano Lett.* **2017**, *17* (10), 6496–6500.
- (39) Ochmann, S. E.; Vietz, C.; Trofymchuk, K.; Acuna, G. P.; Lalkens, B.; Tinnefeld, P. Optical Nanoantenna for Single Molecule-Based Detection of Zika Virus Nucleic Acids without Molecular Multiplication. *Anal. Chem.* **2017**, *89* (23), 13000–13007.
- (40) Kaminska, I.; Bohlen, J.; Mackowski, S.; Tinnefeld, P.; Acuna, G. P. Strong Plasmonic Enhancement of a Single Peridinin-Chlorophyll *a*-Protein Complex on DNA Origami-Based Optical Antennas. *ACS Nano* **2018**, *12* (2), 1650–1655.
- (41) Trofymchuk, K.; Glembockyte, V.; Grabenhorst, L.; Steiner, F.; Vietz, C.; Close, C.; Pfeiffer, M.; Richter, L.; Schütte, M. L.; Selbach, F.; et al. Addressable Nanoantennas with Cleared Hotspots for Single-Molecule Detection on a Portable Smartphone Microscope. *Nat. Commun.* **2021**, *12*, 950.
- (42) Schreiber, R.; Do, J.; Roller, E.-M.; Zhang, T.; Schüller, V. J.; Nickels, P. C.; Feldmann, J.; Liedl, T. Hierarchical Assembly of Metal Nanoparticles, Quantum Dots and Organic Dyes Using DNA Origami Scaffolds. *Nat. Nanotechnol.* **2014**, *9* (1), 74–78.
- (43) Wei, Q.; Acuna, G.; Kim, S.; Vietz, C.; Tseng, D.; Chae, J.; Shir, D.; Luo, W.; Tinnefeld, P.; Ozcan, A. Plasmonics Enhanced Smartphone Fluorescence Microscopy. *Sci. Rep.* **2017**, *7* (1), 2124.
- (44) Zhang, T.; Gao, N.; Li, S.; Lang, M. J.; Xu, Q.-H. Single-Particle Spectroscopic Study on Fluorescence Enhancement by Plasmon Coupled Gold Nanorod Dimers Assembled on DNA Origami. *J. Phys. Chem. Lett.* **2015**, *6* (11), 2043–2049.
- (45) Albinsson, B.; Hännestad, J. K.; Börjesson, K. Functionalized DNA Nanostructures for Light Harvesting and Charge Separation. *Coord. Chem. Rev.* **2012**, *256* (21), 2399–2413.
- (46) Hemmig, E. A.; Creatore, C.; Wünsch, B.; Hecker, L.; Mair, P.; Parker, M. A.; Emmott, S.; Tinnefeld, P.; Keyser, U. F.; Chin, A. W. Programming Light-Harvesting Efficiency Using DNA Origami. *Nano Lett.* **2016**, *16* (4), 2369–2374.
- (47) Kerker, M.; Wang, D.-S.; Chew, H. Surface Enhanced Raman Scattering (SERS) by Molecules Adsorbed at Spherical Particles. *Appl. Opt.* **1980**, *19* (19), 3373–3388.
- (48) Krajczewski, J.; Kołataj, K.; Kudelski, A. Plasmonic Nanoparticles in Chemical Analysis. *RSC Adv.* **2017**, *7* (28), 17559–17576.
- (49) Alamehadi, L. M.; Curley, S. M.; Tokranova, N. A.; Tenenbaum, S. A.; Lednev, I. K. Surface Enhanced Raman Spectroscopy for Single Molecule Protein Detection. *Sci. Rep.* **2019**, *9*, 12356.
- (50) Lim, D.-K.; Jeon, K.-S.; Hwang, J.-H.; Kim, H.; Kwon, S.; Suh, Y. D.; Nam, J.-M. Highly Uniform and Reproducible Surface-Enhanced Raman Scattering from DNA-Tailorable Nanoparticles with 1-Nm Interior Gap. *Nat. Nanotechnol.* **2011**, *6* (7), 452–460.
- (51) Prinz, J.; Schreiber, B.; Olejko, L.; Oertel, J.; Rackwitz, J.; Keller, A.; Bald, I. DNA Origami Substrates for Highly Sensitive Surface-Enhanced Raman Scattering. *J. Phys. Chem. Lett.* **2013**, *4* (23), 4140–4145.
- (52) Thacker, V. V.; Herrmann, L. O.; Sigle, D. O.; Zhang, T.; Liedl, T.; Baumberg, J. J.; Keyser, U. F. DNA Origami Based Assembly of Gold Nanoparticle Dimers for Surface-Enhanced Raman Scattering. *Nat. Commun.* **2014**, *5* (1), 3448.
- (53) Kühler, P.; Roller, E.-M.; Schreiber, R.; Liedl, T.; Lohmüller, T.; Feldmann, J. Plasmonic DNA-Origami Nanoantennas for Surface-Enhanced Raman Spectroscopy. *Nano Lett.* **2014**, *14* (5), 2914–2919.
- (54) Prinz, J.; Heck, C.; Ellerik, L.; Merk, V.; Bald, I. DNA Origami Based Au-Ag-Core-Shell Nanoparticle Dimers with Single-Molecule SERS Sensitivity. *Nanoscale* **2016**, *8* (10), 5612–5620.
- (55) Simoncelli, S.; Roller, E.-M.; Urban, P.; Schreiber, R.; Turberfield, A. J.; Liedl, T.; Lohmüller, T. Quantitative Single-Molecule Surface-Enhanced Raman Scattering by Optothermal Tuning of DNA Origami-Assembled Plasmonic Nanoantennas. *ACS Nano* **2016**, *10* (11), 9809–9815.
- (56) Heck, C.; Kanehira, Y.; Kneipp, J.; Bald, I. Placement of Single Proteins within the SERS Hot Spots of Self-Assembled Silver Nanolenses. *Angew. Chem., Int. Ed.* **2018**, *57* (25), 7444–7447.
- (57) Zhan, P.; Wen, T.; Wang, Z.; He, Y.; Shi, J.; Wang, T.; Liu, X.; Lu, G.; Ding, B. DNA Origami Directed Assembly of Gold Bowtie Nanoantennas for Single-Molecule Surface-Enhanced Raman Scattering. *Angew. Chem., Int. Ed.* **2018**, *57* (11), 2846–2850.
- (58) Zhao, M.-Z.; Wang, X.; Xing, Y.-K.; Ren, S.-K.; Teng, N.; Wang, J.; Chao, J.; Wang, L.-H. DNA Origami-Templated Assembly of Plasmonic Nanostructures with Enhanced Raman Scattering. *Nucl. Sci. Tech.* **2018**, *29* (1), 6.
- (59) Ren, S.; Wang, J.; Song, C.; Li, Q.; Yang, Y.; Teng, N.; Su, S.; Zhu, D.; Huang, W.; Chao, J.; et al. Single-Step Organization of Plasmonic Gold Metamaterials with Self-Assembled DNA Nanostructures. *Research* **2019**, *2019*. DOI: 10.34133/2019/7403580.
- (60) Zhou, C.; Yang, Y.; Li, H.; Gao, F.; Song, C.; Yang, D.; Xu, F.; Liu, N.; Ke, Y.; Su, S.; et al. Programming Surface-Enhanced Raman

Scattering of DNA Origami-Templated Metamolecules. *Nano Lett.* **2020**, *20* (5), 3155–3159.

(61) Moeinian, A.; Gür, F. N.; Gonzalez-Torres, J.; Zhou, L.; Murugesan, V. D.; Dashtestani, A. D.; Guo, H.; Schmidt, T. L.; Strehle, S. Highly Localized SERS Measurements Using Single Silicon Nanowires Decorated with DNA Origami-Based SERS Probe. *Nano Lett.* **2019**, *19* (2), 1061–1066.

(62) Fang, W.; Jia, S.; Chao, J.; Wang, L.; Duan, X.; Liu, H.; Li, Q.; Zuo, X.; Wang, L.; Wang, L. et al. Quantizing Single-Molecule Surface-Enhanced Raman Scattering with DNA Origami Metamolecules. *Sci. Adv.* **2019**, *5* (9). DOI: 10.1126/sciadv.aau4506.

(63) Reguera, J.; Langer, J.; Jimenez de Aberasturi, D.; Liz-Marzan, L. M. Anisotropic Metal Nanoparticles for Surface Enhanced Raman Scattering. *Chem. Soc. Rev.* **2017**, *46* (13), 3866–3885.

(64) Tanwar, S.; Haldar, K. K.; Sen, T. DNA Origami Directed Au Nanostar Dimers for Single-Molecule Surface-Enhanced Raman Scattering. *J. Am. Chem. Soc.* **2017**, *139* (48), 17639–17648.

(65) Ma, W.; Xu, L.; Wang, L.; Xu, C.; Kuang, H. Chirality-Based Biosensors. *Adv. Funct. Mater.* **2019**, *29* (1), 1805512.

(66) Neubrech, F.; Hentschel, M.; Liu, N. Reconfigurable Plasmonic Chirality: Fundamentals and Applications. *Adv. Mater.* **2020**, *32*, 1905640.

(67) *Circular Dichroism and the Conformational Analysis of Biomolecules*; Fasman, G. D., Ed.; Springer: United States, 1996; DOI: 10.1007/978-1-4757-2508-7.

(68) Fan, Z.; Govorov, A. O. Plasmonic Circular Dichroism of Chiral Metal Nanoparticle Assemblies. *Nano Lett.* **2010**, *10* (7), 2580–2587.

(69) Kuzyk, A.; Schreiber, R.; Fan, Z.; Pardatscher, G.; Roller, E.-M.; Högele, A.; Simmel, F. C.; Govorov, A. O.; Liedl, T. DNA-Based Self-Assembly of Chiral Plasmonic Nanostructures with Tailored Optical Response. *Nature* **2012**, *483* (7389), 311–314.

(70) Schreiber, R.; Luong, N.; Fan, Z.; Kuzyk, A.; Nickels, P. C.; Zhang, T.; Smith, D. M.; Yurke, B.; Kuang, W.; Govorov, A. O.; et al. Chiral Plasmonic DNA Nanostructures with Switchable Circular Dichroism. *Nat. Commun.* **2013**, *4* (1), 2948.

(71) Lieberman, I.; Shemer, G.; Fried, T.; Kosower, E. M.; Markovich, G. Plasmon-Resonance-Enhanced Absorption and Circular Dichroism. *Angew. Chem., Int. Ed.* **2008**, *47* (26), 4855–4857.

(72) Kneer, L. M.; Roller, E.-M.; Besteiro, L. V.; Schreiber, R.; Govorov, A. O.; Liedl, T. Circular Dichroism of Chiral Molecules in DNA-Assembled Plasmonic Hotspots. *ACS Nano* **2018**, *12* (9), 9110–9115.

(73) Shen, X.; Song, C.; Wang, J.; Shi, D.; Wang, Z.; Liu, N.; Ding, B. Rolling Up Gold Nanoparticle-Dressed DNA Origami into Three-Dimensional Plasmonic Chiral Nanostructures. *J. Am. Chem. Soc.* **2012**, *134* (1), 146–149.

(74) Yan, W.; Xu, L.; Xu, C.; Ma, W.; Kuang, H.; Wang, L.; Kotov, N. A. Self-Assembly of Chiral Nanoparticle Pyramids with Strong R/S Optical Activity. *J. Am. Chem. Soc.* **2012**, *134* (36), 15114–15121.

(75) Shen, X.; Asenjo-Garcia, A.; Liu, Q.; Jiang, Q.; García de Abajo, F. J.; Liu, N.; Ding, B. Three-Dimensional Plasmonic Chiral Tetramers Assembled by DNA Origami. *Nano Lett.* **2013**, *13* (5), 2128–2133.

(76) Urban, M. J.; Dutta, P. K.; Wang, P.; Duan, X.; Shen, X.; Ding, B.; Ke, Y.; Liu, N. Plasmonic Toroidal Metamolecules Assembled by DNA Origami. *J. Am. Chem. Soc.* **2016**, *138* (17), 5495–5498.

(77) Lan, X.; Lu, X.; Shen, C.; Ke, Y.; Ni, W.; Wang, Q. Au Nanorod Helical Superstructures with Designed Chirality. *J. Am. Chem. Soc.* **2015**, *137* (1), 457–462.

(78) Shen, C.; Lan, X.; Zhu, C.; Zhang, W.; Wang, L.; Wang, Q. Spiral Patterning of Au Nanoparticles on Au Nanorod Surface to Form Chiral AuNR@AuNP Helical Superstructures Templated by DNA Origami. *Adv. Mater.* **2017**, *29* (16). DOI: 10.1002/adma.201606533.

(79) Lan, X.; Liu, T.; Wang, Z.; Govorov, A. O.; Yan, H.; Liu, Y. DNA-Guided Plasmonic Helix with Switchable Chirality. *J. Am. Chem. Soc.* **2018**, *140* (37), 11763–11770.

(80) Wang, M.; Dong, J.; Zhou, C.; Xie, H.; Ni, W.; Wang, S.; Jin, H.; Wang, Q. Reconfigurable Plasmonic Diastereomers Assembled by DNA Origami. *ACS Nano* **2019**, *13* (12), 13702–13708.

(81) Kuzyk, A.; Schreiber, R.; Zhang, H.; Govorov, A. O.; Liedl, T.; Liu, N. Reconfigurable 3D Plasmonic Metamolecules. *Nat. Mater.* **2014**, *13* (9), 862.

(82) Kuzyk, A.; Yang, Y.; Duan, X.; Stoll, S.; Govorov, A. O.; Sugiyama, H.; Endo, M.; Liu, N. A Light-Driven Three-Dimensional Plasmonic Nanosystem That Translates Molecular Motion into Reversible Chiroptical Function. *Nat. Commun.* **2016**, *7* (1), 10591.

(83) Liu, Q.; Kuzyk, A.; Endo, M.; Smalyukh, I. I. Colloidal Plasmonic DNA-Origami with Photo-Switchable Chirality in Liquid Crystals. *Opt. Lett.* **2019**, *44* (11), 2831–2834.

(84) Jiang, Q.; Liu, Q.; Shi, Y.; Wang, Z.-G.; Zhan, P.; Liu, J.; Liu, C.; Wang, H.; Shi, X.; Zhang, L.; et al. Stimulus-Responsive Plasmonic Chiral Signals of Gold Nanorods Organized on DNA Origami. *Nano Lett.* **2017**, *17* (11), 7125–7130.

(85) Kuzyk, A.; Urban, M. J.; Idili, A.; Ricci, F.; Liu, N. Selective Control of Reconfigurable Chiral Plasmonic Metamolecules. *Sci. Adv.* **2017**, *3* (4), No. e1602803.

(86) Man, T.; Ji, W.; Liu, X.; Zhang, C.; Li, L.; Pei, H.; Fan, C. Chiral Metamolecules with Active Plasmonic Transition. *ACS Nano* **2019**, *13* (4), 4826–4833.

(87) Zhou, C.; Xin, L.; Duan, X.; Urban, M. J.; Liu, N. Dynamic Plasmonic System That Responds to Thermal and Aptamer-Target Regulations. *Nano Lett.* **2018**, *18* (11), 7395–7399.

(88) Huang, Y.; Nguyen, M.-K.; Natarajan, A. K.; Nguyen, V. H.; Kuzyk, A. A DNA Origami-Based Chiral Plasmonic Sensing Device. *ACS Appl. Mater. Interfaces* **2018**, *10* (S1), 44221–44225.

(89) Funck, T.; Liedl, T.; Bae, W. Dual Aptamer-Functionalized 3D Plasmonic Metamolecule for Thrombin Sensing. *Appl. Sci.* **2019**, *9* (15), 3006.

(90) Zhou, C.; Duan, X.; Liu, N. A Plasmonic Nanorod That Walks on DNA Origami. *Nat. Commun.* **2015**, *6* (1), 8102.

(91) Funck, T.; Nicoli, F.; Kuzyk, A.; Liedl, T. Sensing Picomolar Concentrations of RNA Using Switchable Plasmonic Chirality. *Angew. Chem.* **2018**, *130* (41), 13683–13686.

(92) Dong, J.; Wang, M.; Zhou, Y.; Zhou, C.; Wang, Q. DNA-Based Adaptive Plasmonic Logic Gates. *Angew. Chem., Int. Ed.* **2020**, *59* (35), 15038–15042.

(93) Urban, M. J.; Zhou, C.; Duan, X.; Liu, N. Optically Resolving the Dynamic Walking of a Plasmonic Walker Couple. *Nano Lett.* **2015**, *15* (12), 8392–8396.

(94) Xin, L.; Zhou, C.; Duan, X.; Liu, N. A Rotary Plasmonic Nanoclock. *Nat. Commun.* **2019**, *10* (1), 5394.

(95) Urban, M. J.; Both, S.; Zhou, C.; Kuzyk, A.; Lindfors, K.; Weiss, T.; Liu, N. Gold Nanocrystal-Mediated Sliding of Doublet DNA Origami Filaments. *Nat. Commun.* **2018**, *9* (1), 1454.

(96) Govorov, A. O.; Fan, Z.; Hernandez, P.; Slocik, J. M.; Naik, R. R. Theory of Circular Dichroism of Nanomaterials Comprising Chiral Molecules and Nanocrystals: Plasmon Enhancement, Dipole Interactions, and Dielectric Effects. *Nano Lett.* **2010**, *10* (4), 1374–1382.

(97) Hendry, E.; Carpy, T.; Johnston, J.; Popland, M.; Mikhaylovskiy, R. V.; Lapthorn, A. J.; Kelly, S. M.; Barron, L. D.; Gadegaard, N.; Kadodwala, M. Ultrasensitive Detection and Characterization of Biomolecules Using Superchiral Fields. *Nat. Nanotechnol.* **2010**, *5* (11), 783–787.

(98) Slocik, J. M.; Govorov, A. O.; Naik, R. R. Plasmonic Circular Dichroism of Peptide-Functionalized Gold Nanoparticles. *Nano Lett.* **2011**, *11* (2), 701–705.

(99) Maoz, B. M.; Chaikin, Y.; Tesler, A. B.; Bar Elli, O.; Fan, Z.; Govorov, A. O.; Markovich, G. Amplification of Chiroptical Activity of Chiral Biomolecules by Surface Plasmons. *Nano Lett.* **2013**, *13* (3), 1203–1209.

(100) Nesterov, M. L.; Yin, X.; Schäferling, M.; Giessen, H.; Weiss, T. The Role of Plasmon-Generated Near Fields for Enhanced Circular Dichroism Spectroscopy. *ACS Photonics* **2016**, *3* (4), 578–583.

- (101) Schlichthaerle, T.; Strauss, M. T.; Schueder, F.; Woehrstein, J. B.; Jungmann, R. DNA Nanotechnology and Fluorescence Applications. *Curr. Opin. Biotechnol.* **2016**, *39*, 41–47.
- (102) Samanta, A.; Banerjee, S.; Liu, Y. DNA Nanotechnology for Nanophotonic Applications. *Nanoscale* **2015**, *7* (6), 2210–2220.
- (103) Pilo-Pais, M.; Acuna, G. P.; Tinnefeld, P.; Liedl, T. Sculpting Light by Arranging Optical Components with DNA Nanostructures. *MRS Bull.* **2017**, *42* (12), 936–942.
- (104) Liu, N.; Liedl, T. DNA-Assembled Advanced Plasmonic Architectures. *Chem. Rev.* **2018**, *118* (6), 3032–3053.
- (105) Ding, B.; Deng, Z.; Yan, H.; Cabrini, S.; Zuckermann, R. N.; Bokor, J. Gold Nanoparticle Self-Similar Chain Structure Organized by DNA Origami. *J. Am. Chem. Soc.* **2010**, *132* (10), 3248–3249.
- (106) Tian, Y.; Wang, T.; Liu, W.; Xin, H. L.; Li, H.; Ke, Y.; Shih, W. M.; Gang, O. Prescribed Nanoparticle Cluster Architectures and Low-Dimensional Arrays Built Using Octahedral DNA Origami Frames. *Nat. Nanotechnol.* **2015**, *10* (7), 637–644.
- (107) Liu, W.; Li, L.; Yang, S.; Gao, J.; Wang, R. Self-Assembly of Heterogeneously Shaped Nanoparticles into Plasmonic Metamolecules on DNA Origami. *Chem. - Eur. J.* **2017**, *23* (57), 14177–14181.
- (108) Liu, W.; Halverson, J.; Tian, Y.; Tkachenko, A. V.; Gang, O. Self-Organized Architectures from Assorted DNA-Framed Nanoparticles. *Nat. Chem.* **2016**, *8* (9), 867–873.
- (109) Gür, F. N.; McPolin, C. P. T.; Raza, S.; Mayer, M.; Roth, D. J.; Steiner, A. M.; Löffler, M.; Fery, A.; Brongersma, M. L.; Zayats, A. V.; et al. DNA-Assembled Plasmonic Waveguides for Nanoscale Light Propagation to a Fluorescent Nanodiamond. *Nano Lett.* **2018**, *18* (11), 7323–7329.
- (110) Liu, M.; Guyot-Sionnest, P.; Lee, T.-W.; Gray, S. K. Optical Properties of Rodlike and Bipyrmidal Gold Nanoparticles from Three-Dimensional Computations. *Phys. Rev. B: Condens. Matter Mater. Phys.* **2007**, *76* (23), 235428.
- (111) Godonoga, M.; Lin, T.-Y.; Oshima, A.; Sumitomo, K.; Tang, M. S. L.; Cheung, Y.-W.; Kinghorn, A. B.; Dirkzwager, R. M.; Zhou, C.; Kuzuya, A.; et al. DNA Aptamer Recognising a Malaria Protein Biomarker Can Function as Part of a DNA Origami Assembly. *Sci. Rep.* **2016**, *6* (1), 21266.
- (112) Bell, N. A. W.; Keyser, U. F. Digitally Encoded DNA Nanostructures for Multiplexed, Single-Molecule Protein Sensing with Nanopores. *Nat. Nanotechnol.* **2016**, *11* (7), 645–651.
- (113) Shaw, A.; Hoffecker, I. T.; Smyraki, I.; Rosa, J.; Grevys, A.; Bratlie, D.; Sandlie, I.; Michaelsen, T. E.; Andersen, J. T.; Högberg, B. Binding to Nanopatterned Antigens Is Dominated by the Spatial Tolerance of Antibodies. *Nat. Nanotechnol.* **2019**, *14* (2), 184–190.
- (114) Zhang, P.; Liu, X.; Liu, P.; Wang, F.; Ariyama, H.; Ando, T.; Lin, J.; Wang, L.; Hu, J.; Li, B.; et al. Capturing Transient Antibody Conformations with DNA Origami Epitopes. *Nat. Commun.* **2020**, *11* (1), 3114.
- (115) Nguyen, L.; Dass, M.; Ober, M. F.; Besteiro, L. V.; Wang, Z. M.; Nickel, B.; Govorov, A. O.; Liedl, T.; Heuer-Jungemann, A. Chiral Assembly of Gold-Silver Core-Shell Plasmonic Nanorods on DNA Origami with Strong Optical Activity. *ACS Nano* **2020**, *14* (6), 7454–7461.
- (116) Zhang, Q.; Hernandez, T.; Smith, K. W.; Hosseini Jebeli, S. A.; Dai, A. X.; Warning, L.; Baiyasi, R.; McCarthy, L. A.; Guo, H.; Chen, D.-H.; et al. Unraveling the Origin of Chirality from Plasmonic Nanoparticle-Protein Complexes. *Science* **2019**, *365* (6460), 1475–1478.
- (117) Vietz, C.; Schütte, M. L.; Wei, Q.; Richter, L.; Lalkens, B.; Ozcan, A.; Tinnefeld, P.; Acuna, G. P. Benchmarking Smartphone Fluorescence-Based Microscopy with DNA Origami Nanobeads: Reducing the Gap toward Single-Molecule Sensitivity. *ACS Omega* **2019**, *4* (1), 637–642.
- (118) Agarwal, N. P.; Matthies, M.; Gür, F. N.; Osada, K.; Schmidt, T. L. Block Copolymer Micellization as a Protection Strategy for DNA Origami. *Angew. Chem., Int. Ed.* **2017**, *56* (20), 5460–5464.
- (119) Hahn, J.; Wickham, S. F. J.; Shih, W. M.; Perrault, S. D. Addressing the Instability of DNA Nanostructures in Tissue Culture. *ACS Nano* **2014**, *8* (9), 8765–8775.
- (120) Kielar, C.; Xin, Y.; Shen, B.; Kostianen, M. A.; Grundmeier, G.; Linko, V.; Keller, A. On the Stability of DNA Origami Nanostructures in Low-Magnesium Buffers. *Angew. Chem., Int. Ed.* **2018**, *57* (30), 9470–9474.
- (121) Nguyen, L.; Döblinger, M.; Liedl, T.; Heuer-Jungemann, A. DNA-Origami-Templated Silica Growth by Sol-Gel Chemistry. *Angew. Chem., Int. Ed.* **2019**, *58* (3), 912–916.
- (122) Wang, S.-T.; Gray, M. A.; Xuan, S.; Lin, Y.; Byrnes, J.; Nguyen, A. I.; Todorova, N.; Stevens, M. M.; Bertozzi, C. R.; Zuckermann, R. N.; et al. DNA Origami Protection and Molecular Interfacing through Engineered Sequence-Defined Peptoids. *Proc. Natl. Acad. Sci. U. S. A.* **2020**, *117* (12), 6339–6348.
- (123) Gerling, T.; Kube, M.; Kick, B.; Dietz, H. Sequence-Programmable Covalent Bonding of Designed DNA Assemblies. *Sci. Adv.* **2018**, *4* (8), No. eaau1157.
- (124) Cassinelli, V.; Oberleitner, B.; Sobotta, J.; Nickels, P.; Grossi, G.; Kempter, S.; Frischmuth, T.; Liedl, T.; Manetto, A. One-Step Formation of “Chain-Armor”-Stabilized DNA Nanostructures. *Angew. Chem., Int. Ed.* **2015**, *54* (27), 7795–7798.
- (125) Ke, Y.; Ong, L. L.; Sun, W.; Song, J.; Dong, M.; Shih, W. M.; Yin, P. DNA Brick Crystals with Prescribed Depths. *Nat. Chem.* **2014**, *6* (11), 994–1002.
- (126) Tian, Y.; Zhang, Y.; Wang, T.; Xin, H. L.; Li, H.; Gang, O. Lattice Engineering through Nanoparticle-DNA Frameworks. *Nat. Mater.* **2016**, *15* (6), 654–661.
- (127) Liu, W.; Tagawa, M.; Xin, H. L.; Wang, T.; Emamy, H.; Li, H.; Yager, K. G.; Starr, F. W.; Tkachenko, A. V.; Gang, O. Diamond Family of Nanoparticle Superlattices. *Science* **2016**, *351* (6273), 582–586.
- (128) Zhang, T.; Hartl, C.; Frank, K.; Heuer-Jungemann, A.; Fischer, S.; Nickels, P. C.; Nickel, B.; Liedl, T. 3D DNA Origami Crystals. *Adv. Mater.* **2018**, *30* (28), 1800273.
- (129) Praetorius, F.; Kick, B.; Behler, K. L.; Honemann, M. N.; Weuster-Botz, D.; Dietz, H. Biotechnological Mass Production of DNA Origami. *Nature* **2017**, *552* (7683), 84–87.